LANGMUIR Article
Cite This: Langmuir 2019, 35, 10601−10609
pubs.acs.org/Langmuir

Antibodies Irreversibly Adsorb to Gold Nanoparticles and Resist Displacement by Common Blood Proteins

Guadalupe Ruiz, Nicki Ryan, Kylie Rutschke, Olatunde Awotunde, and Jeremy D. Driskell*

Department of Chemistry, Illinois State University, Normal, Illinois 61790, United States

Supporting Information

ABSTRACT: Gold nanoparticles (AuNPs) functionalized with proteins to impart desirable surface properties have been developed for many nanobiotechnology applications. A strong interaction between the protein and nanoparticle is critical to the formation of a stable conjugate to realize the potential of these emerging technologies. In this work, we examine the robustness of a protein layer adsorbed onto gold nanoparticles while under the stress of a physiological environment that could potentially lead to protein exchange on the nanoparticle surface. The adsorption interaction of common blood plasma proteins (transferrin, human serum albumin, and fibrinogen) and anti-horseradish peroxidase antibody onto AuNPs is investigated by nanoparticle tracking analysis. Our data show that a monolayer of protein is formed at saturation for each protein, and the maximum size increase for the conjugate, relative to the AuNP core, correlates with the protein size. The binding affinity of each protein to the AuNP is extracted from a best fit of the adsorption isotherm to the Hill equation. The antibody displays the greatest affinity (K_d = 15.2 ± 0.8 nM) that is ∼20−65 times stronger than the affinity of the other plasma proteins. Antibody−AuNP conjugates were prepared, purified, and suspended in solutions of blood plasma proteins to evaluate the stability of the antibody layer. An enzyme-mediated assay confirms that the antibody−AuNP interaction is irreversible, and the adsorbed antibody resists displacement by the plasma proteins. This work provides insight into the capabilities and potential limitations of antibody−AuNP-enabled technologies in biological systems.

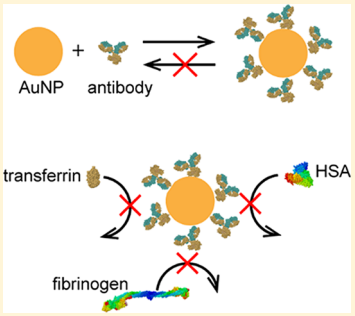

INTRODUCTION

Synthesis of engineered nanoparticles with a well-controlled surface chemistry is critical to the development of transformative technologies for biomedical applications,[1−4] including imaging,[5,6] drug delivery,[7] photothermal therapy,[8] and diagnostic testing.[9] The interfacial chemistry of nanoparticles can be tailored to provide application-specific needs such as cellular uptake,[10,11] low toxicity,[12,13] stealth-like properties,[14−17] and targeted binding.[18] Despite the engineering controls used to produce the nanoparticle surface chemistry, it is well established that proteins readily adsorb onto nanoparticles upon introduction into a biological fluid to form a protein corona.[19−22] Consequently, the corona can modulate the interfacial chemistry and alter the intended functionality.[23−25] Thus, it is imperative to characterize the protein corona and investigate the impact of the corona on the nanoparticle as it relates to the downstream application.

A growing body of work has shown that the composition of the protein corona depends on the nanoparticle surface chemistry, curvature, and composition of the suspending matrix.[26−28] Several reports have found that the corona composition is dynamic in which the corona is initially formed with the most abundant matrix proteins yet evolves over time to be dominated by the proteins with the greatest binding affinity for the nanoparticle.[27,29] In contrast, other groups have observed irreversible protein binding to nanoparticles.[30−32] These differences in adsorption dynamics can be attributed to the complexity of the protein−nanoparticle interaction that lead to system-dependent outcomes. Ultimately, these works highlight the need to study each nanoparticle and protein system independently.

To improve the stability of the engineered protein layer on nanoparticles, chemical linkers are often utilized to covalently attach proteins. One commonly employed approach is to use activated ester-functionalized nanoparticles to covalently bond proteins through the amine moiety of the lysine residue.[33−38] While this strategy is appropriate for coupling proteins to many types of nanoparticles, it may not be necessary for coupling to gold nanoparticles. Several groups have observed similar coupling of proteins to gold nanoparticles prepared via spontaneous adsorption and NHS/EDC coupling chemistry.[39−41] A recent work probing the adsorption of immunoglobulin G, bovine serum albumin, site-directed cysteine mutants of pyrophosphatase, and GB3 mutants with varying numbers of cysteine residues suggests that proteins chemisorb to gold nanoparticles through the formation of Au−S bond between cysteine and the gold nanoparticle.[30−32,42−44] Evidence for the strong interaction between cysteine-containing proteins and gold nanoparticles includes resistance of the protein adlayer to displacement by small organothiols.[31,43] In this work, we aim to evaluate the susceptibility of antibody adsorbed onto gold nanoparticles to displacement by

Received: June 21, 2019
Revised: July 11, 2019
Published: July 23, 2019

DOI: 10.1021/acs.langmuir.9b01900
Langmuir 2019, 35, 10601−10609

blood plasma proteins when suspended in a physiological matrix.

Our group, as well as others, has recently developed several AuNP-enabled immunoassays that rely on antibody−AuNP conjugates to selectively bind targeted antigens for detection.[41,45−51] These assays mix conjugates with blood serum or allantoic fluid and allow ∼60 min for antigens to bind and cross-link the conjugates. The aggregates can be directly detected via dynamic light scattering (DLS) or captured on size-selective membrane for surface-enhanced Raman spectroscopy analysis. Success of these AuNP-enabled platforms hinges on the robust antibody coating. Consequently, displacement of the antibody on the AuNP by matrix proteins or further protein adsorption to form multilayers has the potential inhibit antigen-mediated aggregation of the conjugates. In this work, we preadsorb antibody onto AuNPs, purify the conjugate, then assess displacement by the most abundant plasma proteins, for example, human serum albumin (HSA), transferrin, and fibrinogen, and whole serum. This study to kinetically monitor the disruption of the antibody−AuNP interaction by plasma proteins defines the capabilities and potential limitations to downstream biomedical applications.

EXPERIMENTAL SECTION

Reagents. All studies were conducted using citrate-capped, spherical gold nanoparticles (AuNPs) purchased from Ted Pella Inc. (Redding, CA) with a nominal diameter of 60 nm. The hydrodynamic diameter of the AuNPs measured was 62.1 ± 0.6 nm via nanoparticle tracking analysis with a zeta potential of −43 ± 1 mV. Mouse anti-HRP IgG monoclonal antibody (clone 2H11, 5.3 mg/mL) was obtained from BioSource. Goat antimouse IgG polyclonal antibody (1.1 mg/mL) was obtained from Abcam. The blood plasma proteins, human serum albumin (HSA), fibrinogen, and transferrin were all obtained from Sigma-Aldrich (St. Louis, MO). Normal human serum, horseradish peroxidase (HRP), and 2,2′-azino-bis(3-ethylbenzothiazoline-6-sulfonic acid (1-Step ABTS) were purchased from Thermo Scientific (Rockford, IL). Potassium phosphate monohydrate was acquired from Fisher Scientific (Fair Lawn, NJ), and anhydrous potassium phosphate dibasic was purchased from Mallinckrodt Chemicals, Inc. (Paris, KY). To achieve the correct pH, NaOH and HCl were added to phosphate buffer. A Barnstead water purification system (Thermo Scientific, Rockford, IL) provided nanopure deionized water (18 MΩ) and was used to prepare all aqueous solutions.

Protein Adsorption Isotherm. AuNPs (60 nm, 100 μL) were added into a low binding microcentrifuge tube, and 4 μL of 50 mM phosphate buffer (pH 7.5) was added to adjust the pH. Varying concentrations (final protein concentrations) of mouse anti-HRP antibody (0−310 nM), HSA (0−50,000 nM), fibrinogen (0−10,000 nM), and transferrin (0−5,000 nM) were added to the AuNP suspensions. All protein−AuNP conjugate suspensions were left to incubate for 1 h at room temperature. After incubation with protein, 10 μL of the functionalized AuNPs was diluted in 990 μL of 2 mM phosphate buffer (pH 7.5) and analyzed using nanoparticle tracking analysis (NTA) to measure the hydrodynamic diameter of the conjugates. This process was repeated for each blood plasma protein and concentration.

Quantifying Antibody Displacement by Blood Plasma Proteins. *Preparation of Protein−AuNP Conjugates.* AuNPs (60 nm, 100 μL), 4 μL of 50 mM phosphate buffer (pH 7.5), and 4 μg of anti-HRP antibody were mixed and incubated for 1 h at room temperature in a low binding microcentrifuge tube. Goat antimouse−AuNP conjugates were prepared similarly and served as a negative control to evaluate the nonspecific interaction of HRP with AuNP conjugates. Then, the antibody−AuNP conjugates were centrifuged at 5000 g for 5 min, the supernatant was removed, and the pellet was resuspended with 2 mM phosphate buffer. To ensure removal of excess antibody, this wash process was repeated three additional times. After the final centrifugation, supernatant was removed and replaced with a blood plasma protein at a concentration equal to 10% of the physiological concentration found in normal blood, for example, 60 μM HSA, 1 μM fibrinogen, and 3 μM transferrin, or 10% human serum. Different incubation periods (1−24 h) were used to investigate the displacement of antibody from the antibody−AuNP conjugates by blood plasma proteins.

Quantitation of Anti-HRP Antibody Adsorbed onto AuNP by HRP Enzymatic Reaction. HRP (1 mg/mL, 3 μL) was added to the anti-HRP−AuNP or anti-mouse IgG−AuNP conjugates mixed with blood plasma protein and incubated for 1 h. This allows for complete saturation of all accessible antigen binding sites of the antibodies. Then, the samples were centrifuged at 5000 g for the HSA, fibrinogen, and transferrin sample and at 17,000 g for the serum sample. A greater centrifugation rate was required to pellet the conjugate in the serum sample, presumably due to greater viscosity of serum. The supernatant was removed, and the pellet was resuspended in 2 mM phosphate buffer. The washes were repeated three additional times to remove any excess HRP or desorbed antibodies in solution. In a 96-well plate, three 10 μL aliquots of each conjugate were placed and mixed with 150 μL of 1-Step ABTS. The kinetics of the enzymatic reaction between HRP and ABTS was monitored by the absorption of the green colored product, oxidized ABTS, at 415 nm for 20 min at 10 s intervals to determine the enzymatic reaction rate. The enzymatic reaction rate was normalized for differences in AuNP concentrations.

Reversibility of Antibody−AuNP Adsorption. AuNPs (60 nm, 100 μL), 4 μL of 50 mM phosphate buffer (pH 7.5), and anti-HRP antibody at a final concentration of 120 nM were mixed and incubated for 1 h at room temperature in a low binding microcentrifuge tube. This concentration of antibody was sufficient to saturate the AuNP with a monolayer of antibody. After incubation with protein, 10 μL of the functionalized AuNPs was diluted in 1.5 mL of 2 mM phosphate buffer (pH 7.5) (1:150 dilution; 0.8 nM antibody) and immediately analyzed using nanoparticle tracking analysis (NTA) to measure the hydrodynamic diameter. The diluted sample was retained for analysis at various time points (t = 1 h, 6 h, 2 days, 3 days, 4 days, and 7 days).

Instrumentation. *Nanoparticle Tracking Analysis (NTA).* A NanoSight LM10 NTA system equipped with an LM14 532 nm laser module and a high sensitivity sCMOS camera was used to measure hydrodynamic diameters of the protein−AuNP conjugates. A syringe pump was interfaced with the sample cell, and the sample was analyzed under a constant flow rate of 15 μL/min to improve sampling. Five 60 s videos, using camera level 9, were collected for each sample and analyzed with the detention threshold set to level 5. These instrumental parameters facilitated the discrete analysis of approximately 10,000 functionalized AuNPs to calculate the mean, mode, and standard deviation of the hydrodynamic diameter for each sample.

UV−Visible Spectrophotometer. Absorbance of the HRP-ABTS enzymatic reaction to obtain the reaction rate was collected using a Bio-Rad iMark Microplate reader set to readout the absorbance at 415 nm at 10 s intervals for 20 min. Spectra of the AuNP conjugates were collected at 0.5 nm intervals over a wavelength range of 400−900 nm using a Cary 1 Bio UV−visible dual-bean spectrophotometer.

RESULTS AND DISCUSSION

Analysis of Protein Adsorption onto Gold Nanoparticles. While there are inconsistencies in studies regarding the formation of a protein corona around a nanoparticle, one commonly observed phenomenon follows the Vroman effect in which small abundant proteins form the initial corona upon introduction of a nanoparticle into a biological fluid, such as blood plasma.[52] However, these small proteins are subsequently replaced over time by the proteins with the greatest affinity for the nanoparticle surface, as expected of equilibrium

DOI: 10.1021/acs.langmuir.9b01900
Langmuir 2019, 35, 10601−10609

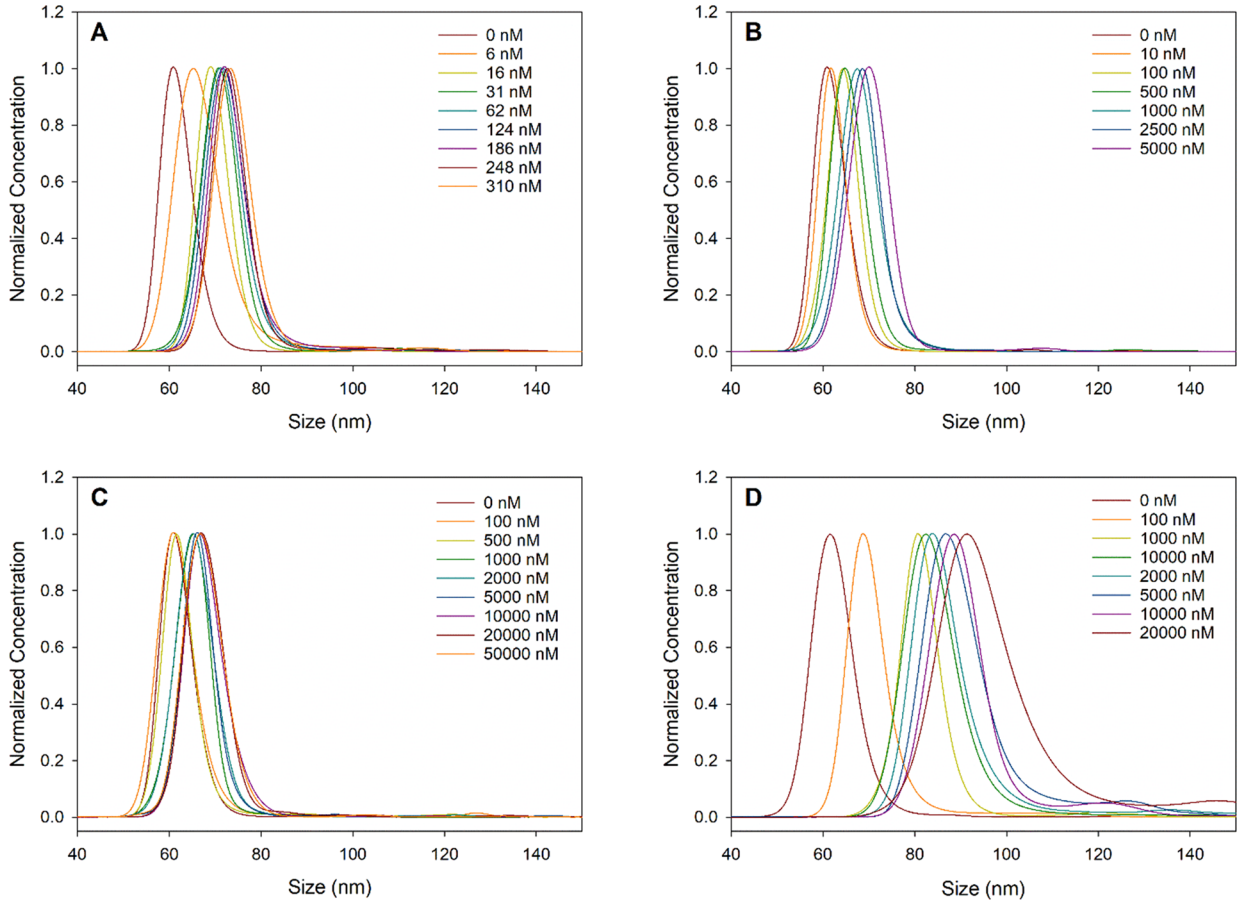

Figure 1. NTA histograms for the size distribution of conjugates formed from the adsorption of proteins as a function of protein concentration: (A) anti-HRP IgG, (B) transferrin, (C) HSA, and (D) fibrinogen.

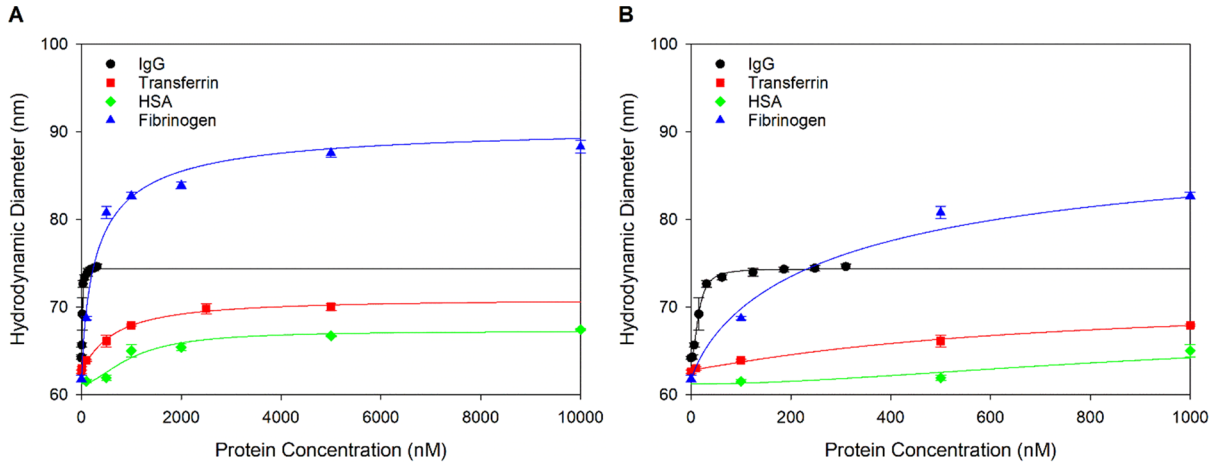

Figure 2. Adsorption of protein onto 60 nm AuNPs as a function of protein concentration. Plots of the mode hydrodynamic diameter of the conjugate as a function of protein concentration. (A) Full range and (B) low concentration range of protein concentrations. The solid curves represent the best fit to the Hill equation (eq 1).

dynamics.[29,53] The objective of this work is to determine the resiliency of antibody−gold nanoparticle conjugates for use in diagnostic assays; thus, it is necessary to begin by measuring the binding affinity of common blood plasma proteins and an IgG antibody. We hypothesized that any plasma protein exhibiting a greater binding affinity to AuNP than the antibody could potentially displace the antibody on the AuNP surface, following the Vroman effect, and ultimately diminish the function of these conjugates in an application, for example, diagnostics, imaging, or targeted drug delivery.

Binding parameters of the most abundant plasma proteins, transferrin, fibrinogen, and human serum albumin (HSA), and an antibody (anti-HRP) are quantitatively assessed using nanoparticle tracking analysis (NTA). NTA provides a measure of the nanoparticle hydrodynamic diameter with subnanometer resolution by tracking the Brownian motion of

DOI: 10.1021/acs.langmuir.9b01900
Langmuir 2019, 35, 10601−10609

individual nanoparticles. Particle-by-particle analysis provides equal weight to each analyzed nanoparticle, eliminating the bias toward larger particles that is commonly observed with ensemble averaging techniques such as dynamic light scattering (DLS).[54−56] NTA readily detects protein adsorption onto gold nanoparticles as an increase in the hydrodynamic diameter, as previously established by our group, to elucidate protein adsorption parameters.[42,55]

The adsorption behavior of IgG, transferrin, HSA, and fibrinogen are determined by adding increasing concentration of each plasma protein to a suspension of AuNPs and measuring the hydrodynamic diameter of the AuNP conjugate. The histograms of size distributions as a function of protein concentration are presented in Figure 1. The hydrodynamic diameter of the population initially shifts to larger sizes with increasing protein concentration, until the protein saturates the AuNP surface at monolayer coverage. Figure 1 shows a highly monodisperse population of conjugates with few, if any, detectable aggregates. Occasionally, an aggregate flows into the field of view to result in a small but detectable increase in the population mean hydrodynamic diameter, effectively reducing the precision of repeat measurements. The mode, however, is unaffected by the observation and analysis of these random aggregates; thus, the conjugate size is reported as the population mode.

Adsorption isotherms are generated for IgG, transferrin, HSA, and fibrinogen to quantitatively define the adsorption behavior of each plasma protein. The hydrodynamic diameter (mode) measured by NTA is plotted as a function of protein concentration and best fit to the Hill equation[20,57,58]

$$D_H = D_{H,initial} + \frac{\Delta D_{H,max}[antibody]^n}{K_d{}^n + [antibody]^n} \quad (1)$$

where D_H is the hydrodynamic diameter, $\Delta D_{H,max}$ is the maximum increase in hydrodynamic diameter resulting from a protein monolayer, n relates to the binding cooperativity, for example, Hill coefficient, and K_d is the dissociation constant for protein−AuNP adsorption (Figure 2). The adsorption interaction between proteins and nanoparticles is often accurately described by the Hill-modified−Langmuir equation. This adsorption model assumes that equilibrium conditions and protein adsorption are limited to monolayer coverage.[20,57,58] The thickness of the protein layer ($\Delta D_{H,max}$), the strength of the protein−AuNP interaction (K_d), and an estimate of binding cooperativity (n) are parameters that can be derived from the best fit of the experimental data to the Hill equation and used to quantitatively compare binding behavior among different proteins.

Table 1 summarizes the characteristic binding parameters extracted from the adsorption isotherms presented in Figure 2. Each protein saturates at monolayer coverage; however, the thickness of the protein monolayer is protein-dependent. At monolayer coverage, the $\Delta D_{H,max}$ measures 6.1 ± 0.8, 8.1 ± 0.8, 10.3 ± 0.3, and 29.5 ± 2.8 nm for HSA (66 kDa), transferrin (78 kDa), IgG (150 kDa), and fibrinogen (340 kDa), respectively (Table 1). The protein layer thickness is dependent on protein orientation,[42,59] which is not controlled in this experiment. Nonetheless, these values are consistent with previously reported $\Delta D_{H,max}$ values for these proteins.[55,58] In general, the thickness of the protein layer correlates with protein size, as anticipated.

Table 1. Adsorption Parameters Determined from Best Fit of NTA Adsorption Isotherm to Hill−Langmuir Model[a]

protein	$\Delta D_{H,max}$ (nm)	K_d (nM)	n
anti-HRP IgG	10.3 ± 0.3	15.2 ± 0.8	2.0 ± 0.2
fibrinogen	29.5 ± 2.8	321 ± 98	0.8 ± 0.2
HSA	6.1 ± 0.8	1008 ± 237	1.8 ± 0.7
transferrin	8.1 ± 0.8	641 ± 126	1.1 ± 0.2

[a]Values represent the average and standard deviation for the analysis of three adsorption datasets for each protein.

The adsorption affinity of each protein for the AuNP is also obtained from the analysis of the adsorption isotherm data with the Hill equation. The adsorption affinity is protein-specific and widely varies. Anti-HRP IgG exhibits the greatest affinity for the AuNP with an observed K_d value of 15.2 ± 0.8 nM (Table 1). This value constitutes a strong interaction between the antibody and AuNP and is consistent with K_d values reported in the literature for IgG−AuNP.[21] HSA displays the weakest affinity for AuNP among the proteins in this work, with a measured K_d value of 1008 ± 237 nM. Previous works have also measured a weaker interaction between HSA and AuNP than IgG, with a typical K_d value of ∼1 uM.[60] Fibrinogen and transferrin show intermediate affinities, with K_d values of 321 ± 98 and 641 ± 126 nM, respectively. The isoelectric point and number of cysteine residues for each protein are provided in Table S1 to identify any correlation between binding affinity and these protein characteristics. While it may be reasonable to anticipate an increase in protein affinity with an increase in cysteine residues, no trend was observed. The cysteines are often involved in disulfide bonding; thus, the total cysteine count does not reflect the number of accessible free sulfhydryl groups responsible for chemisorption to AuNPs. There is a general increase in binding affinity as the protein pI approaches the solution pH of 7.5. However, protein adsorption is a multifaceted process, and pI is not solely responsible for protein binding affinity. Engineered protein mutants with similar pIs exhibited different binding behaviors to AuNPs[31,44] and a single protein displayed equivalent binding affinity to AuNP under different pH conditions;[42] thus, electrostatic interactions, for example, pI, is only one parameter impacting protein binding affinity.

Hill coefficients for each protein adsorption are provided in Table 1. Cooperative binding is observed for IgG, HSA, and transferrin, while anticooperative binding is found for fibrinogen. Given the complexity of the adsorption mechanism and large size of the proteins with several localized regions of positive and negative charges, a detailed interpretation of the Hill coefficient to attribute cooperative or anticooperative behavior to specific interactions is not possible. However, under the experimental conditions, each protein is negatively charged, and adsorption of the protein to the AuNP increases the conjugate zeta potential. We can speculate that this reduction in AuNP charge may be responsible for the cooperative binding found for IgG, HSA, and transferrin. Steric effects resulting from submonolayer formation of fibrinogen may lead to anticooperative binding of subsequent fibrinogen molecules. Alternatively, it is possible that the outward-facing localized regions of charge on the adsorbed proteins influence the attraction/repulsion of subsequent molecules during adsorption.

Competition of Plasma Proteins with Antibody Adsorbed onto Gold Nanoparticles. Typically, the

DOI: 10.1021/acs.langmuir.9b01900
Langmuir 2019, 35, 10601−10609

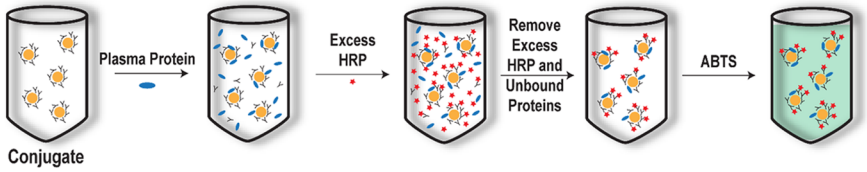

Figure 3. Illustration depicting the enzymatic assay used to quantify protein exchange and displacement of anti-HRP adsorbed onto AuNP by plasma proteins. Purified anti-HRP conjugates are incubated with plasma proteins for a defined period of time to allow protein exchange on the AuNP surface. HRP is added to the suspension to saturate all antibody binding sites. Excess HRP and unbound proteins are separated from the conjugates, and ABTS is added to the conjugates. The enzymatic reaction rate at which HRP catalyzes the oxidation of ABTS quantitatively correlates to the number of HRP molecules captured by the conjugates.

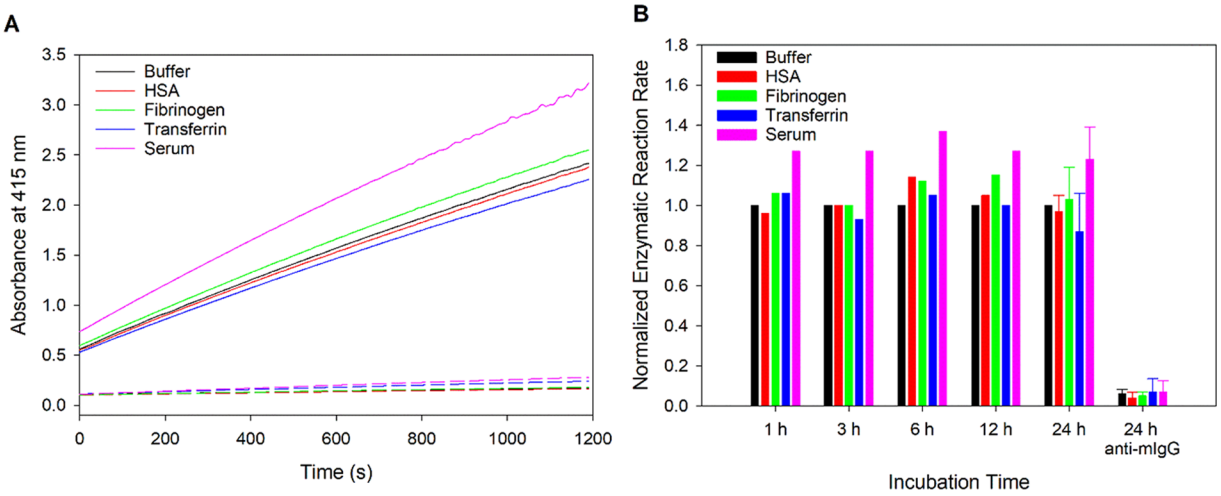

Figure 4. Quantitation of protein exchange. UV−vis kinetic plots of enzymatic reaction rate for the oxidation of ABTS by HRP captured by conjugates. (A) Solid lines represent anti-HRP−AuNP conjugates, and dashed lines represent goat anti-mouse IgG−AuNP conjugates. (B) Normalized reaction rates for HRP captured by conjugates after allowing for potential protein exchange.

composition of the protein corona is studied by competitive binding of a protein mixture to a surface. Under this condition and assuming the Vroman model accurately describes the adsorption of antibodies and plasma proteins, it is reasonable to expect that the corona is primarily dominated by the antibody because IgG possesses the greatest affinity for the AuNP. However, applications involving antibody−AuNP conjugates requires separation of the free IgG from the conjugate. After purification of the conjugate, the system is no longer at equilibrium, and antibody is expected to spontaneously desorb to re-establish equilibrium. Moreover, the high concentration of plasma proteins in the sample matrix will have a greater propensity to compete for binding sites and displace the antibody. Thus, we systematically investigated the potential displacement of antibody from antibody−AuNP conjugates by transferrin, fibrinogen, and HSA, where the antibody was preadsorbed onto the AuNP and the conjugate was separated from the excess free antibody prior to incubation with the plasma proteins.

An enzyme-mediated assay previously employed by our laboratory is slightly modified to quantify the displacement of antibody from the AuNP surface by the plasma proteins (Figure 3).[42,61] Gold nanoparticles are first incubated with excess anti-HRP antibody to fully saturate the AuNP surface. Excess antibody is then separated from the antibody−AuNP conjugates via multiple centrifugation cycles. Plasma protein is then added to the purified conjugate and incubated to allow for potential protein exchange. Excess HRP is added to the suspension to saturate all antibody binding sites, including the free displaced antibody in solution and antibody remaining adsorbed onto the AuNP. The conjugate is then separated from unbound HRP and unbound proteins via centrifugation, and the relative number of HRP molecules captured by the conjugate are quantified by the enzymatic reaction rate of HRP with ABTS. Displacement of the antibody layer by plasma proteins is quantified by a decrease in the enzymatic reaction rate as the conjugates capture fewer HRP molecules. The composition of the protein corona is more commonly determined by chromatography, gel electrophoresis, or mass spectrometry;[19,27] however, these methods cannot differentiate other plasma IgG molecules that may displace the originally adsorbed antibody. The enzymatic assay used here overcomes this limitation and can easily detect the displacement of the antibody from the AuNP surface, even if replaced by another IgG protein.

Our previously optimized protocol for AuNP-enabled immunoassays required 1 h incubation of antibody−AuNP conjugates with a 10-fold dilution of the sample.[41,45,48,50] Any loss of antibody from the AuNP surface will result in diminished analytical performance; thus, it is imperative that the antibody−AuNP conjugates resist degradation, for example, protein exchange, for a minimum of 1 h when suspended in a biological matrix. Guided by these assay parameters, we began by systematically evaluating the ability of individual plasma proteins to displace antibody after 1 h of exposure at 10% of the physiological concentration found in normal blood plasma. Figure 4A shows the enzyme kinetics for HRP captured by the antibody−AuNP conjugates after 1 h

DOI: 10.1021/acs.langmuir.9b01900
Langmuir 2019, 35, 10601−10609

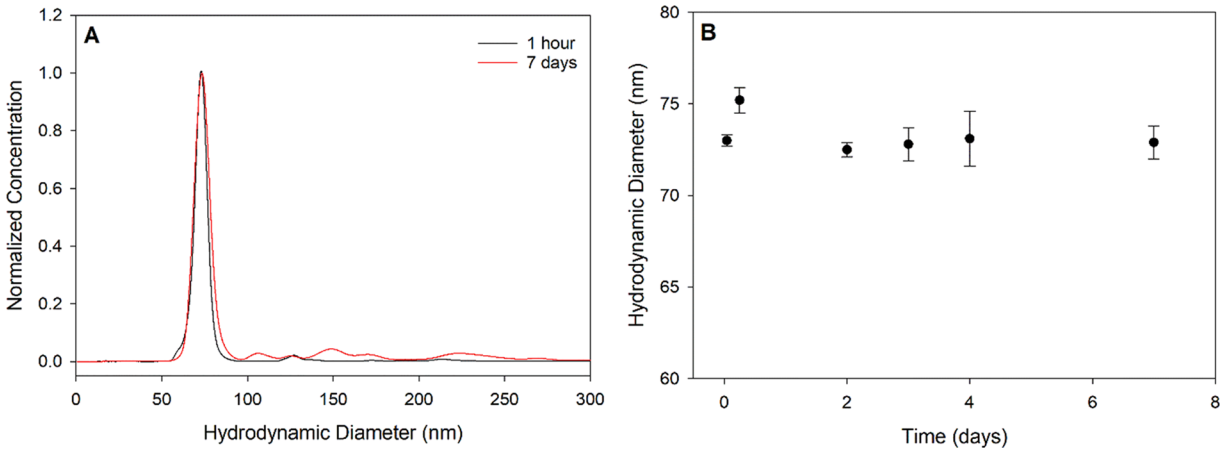

Figure 5. Reversibility of antibody−AuNP interaction. (A) Overlaid NTA histograms for the size distribution of conjugates formed from the addition of 120 nM anti-HRP IgG and collected 1 h and 7 days after 150× dilution. (B) Mode and standard deviation of the hydrodynamic diameter of the diluted conjugates as a function of time.

incubation in a solution of the matrix proteins. As a positive control, the conjugate is incubated in buffer without a competing protein and served as a theoretical maximum rate to which all other rates could be normalized. The data in Figure 4 clearly show no detectable decrease in the reaction rate due to incubation with the individual plasma proteins and suggest that the antibody−AuNP interaction resists protein exchange within the first hour. The conjugates are also mixed with 10% whole human serum for 1 h to evaluate the combined impact of fibrinogen, transferrin, HSA, and all other minor constituents of serum. Interestingly, the reaction rate increases for the HRP-captured conjugates in the serum. This would suggest that serum enhances the binding of HRP to the antibody−AuNP conjugate rather than reducing the binding because of antibody displacement. While not an anticipated result, other groups have reported improved antibody−antigen binding in a serum compared to buffer.[62−64] This is likely due to the presence of complimentary binding proteins or simply better antibody folding and stability in its native environment, for example, serum.[64] The incubation time of the conjugates with the plasma proteins is increased to determine the kinetics of protein displacement, if the antibody is, in fact, displaced. After a maximum incubation time of 24 h, there is no evidence for antibody displacement by the individual plasma proteins, while the serum matrix maintains a similar increase in the enzymatic reaction rate relative to the buffer control regardless of the incubation time (Figure 4B). Considering that the opportunity for antibody displacement increases with incubation time, and there is no evidence for antibody displacement at any incubation time point, only the longest incubation time (24 h) was performed in replicate experiments (N = 4 or 5). A t-test analysis was performed to compare the enzymatic reaction rates for the 24 h incubation data presented in Figure 4B, and no statistical difference is observed between the experimental samples (HSA, fibrinogen, transferrin, and serum) and the positive control (buffer).

It is possible that protein exchange does take place and HRP nonspecifically adsorbs to one of the plasma proteins or that HRP itself displaces the antibody and directly adsorbs onto the AuNP. Either of these cases would lead to an appreciable enzymatic reaction rate and inaccurate conclusion related to the stability of the adsorbed anti-HRP antibody. To evaluate nonspecific binding and potential exchange by HRP, goat anti-mouse IgG−AuNP conjugates are prepared as a negative control. These anti-mIgG−AuNP conjugates do not specifically bind HRP; thus, oxidation of ABTS is unexpected for this negative control, and any appreciable reaction rate for the oxidation of ABTS would be attributed to nonspecific binding of HRP to the AuNP conjugate. These anti-mIgG−AuNP conjugates are incubated in buffer, with each plasma protein, and 10% serum for 24 h to allow for maximum nonspecific binding. Figure 4A,B shows a negligible enzymatic reaction rate and confirms that HRP is binding only to the anti-HRP antibody immobilized on the conjugate. Collectively, these data establish that the antibody−AuNP conjugate is stable for a minimum of 24 h, maintains binding function, and is suitable for applications that are complete in 24 h or less. Moreover, these results indicate that the antibody irreversibly adsorbs onto AuNPs.

Reversibility of Antibody−Gold Nanoparticle Interaction. Results from the protein competition study in the previous section suggest that the antibody irreversibly adsorbs onto the AuNP. To evaluate the reversibility of the antibody−AuNP interaction, AuNPs are mixed with 120 nM antibody for 1 h. This concentration of antibody is sufficient to form a full monolayer on the AuNP surface. The antibody−AuNP mixture is diluted 150-fold to reduce the antibody concentration to 0.8 nM, well below the requisite concentration to saturate the AuNP surface. The hydrodynamic diameter of the diluted antibody−AuNP suspension is monitored over a period of 7 days (Figure 5). The size of the conjugate is expected to decrease if the antibody desorbs from the AuNP surface to re-establish equilibrium, whereas the conjugate size will remain stable if the interaction is irreversible.[30,59] A few aggregates are formed over the 7 day period, as evident in Figure 5A; however, the mode hydrodynamic diameter does not significantly vary after 7 days (Figure 5A,B). Thus, we conclude the antibody−AuNP interaction is irreversible.

The reversibility of protein−nanoparticle adsorption has been shown to vary with the identity of the protein and the nanoparticle.[19,29,59,65,66] Several examples have been reported on the dissociation of proteins from the surface of nanoparticles; it is reported that HSA readily disassociates from quantum dots and several plasma proteins have been found to desorb from polymeric particles. However, our system involves gold nanoparticles and likely benefits from the strong

DOI: 10.1021/acs.langmuir.9b01900
Langmuir 2019, 35, 10601−10609

chemisorption of cysteine residues to the AuNP to irreversibly adsorb. One study recently demonstrated that BSA remains adsorbed onto AuNPs in BSA-free solution for 24 h, and another study found that cysteine-containing proteins irreversibly adsorb onto gold nanoparticles and resist displacement by small organothiols and other thiolated amino acids.[30,31,43] Our data presented here, in addition to these other recent publications, suggest that the antibody is covalently adsorbed onto the AuNP, contradicting the commonly stated belief that protein adsorption arises from hydrophilic, electrostatic, and other noncovalent interactions.[30,31,41−43]

CONCLUSIONS

Here, we find that antibody irreversibly adsorbs onto gold nanoparticles to form robust conjugates. Nanoparticle tracking analysis is used to quantitatively measure the binding affinity of the most abundant plasma proteins to citrate-capped gold nanoparticles, and we find that IgG proteins exhibit the greatest affinity. To evaluate the stability of the AuNP−Ab interaction, purified AuNP−Ab conjugates are mixed with physiological concentrations of plasma proteins, thereby disrupting equilibrium conditions. Interestingly, no displacement of the antibody form the AuNP surface is observed. A subsequent study found that antibody desorption from the AuNP surface is not detectable within 7 days of forming and purifying the conjugate. These data suggest that covalent coupling of antibody to AuNPs with cross-linking reagents is not necessary. Many current practices for nanoparticle modification capitalize on activated esters to covalently link lysine residues on proteins to nanoparticles. This approach is effective, if not required, to form a robust protein layer on polymeric nanoparticles, quantum dots, or other non-gold particles; however, surface functionalization of gold nanoparticles with proteins that display surface accessible cysteine residues may not require the use of covalent coupling agents. Further study is necessary to isolate the point of interaction between the adsorbed proteins and AuNPs. Our studies also demonstrate that the interaction between the antibody and AuNP is irreversible on the timescale of the experiments; thus, fitting the adsorption isotherms to the Hill equation, which assumes equilibrium conditions, may not be strictly valid and only provides a qualitative comparison of relative adsorption affinities among the proteins.[30] Nevertheless, this work establishes the irreversible and robust nature of the antibody−AuNP interaction that allows for biomedical applications of AuNP−Ab conjugates in blood plasma for protocols requiring less than 24 h without concern for diminished performance.

ASSOCIATED CONTENT

Supporting Information

The Supporting Information is available free of charge on the ACS Publications website at DOI: 10.1021/acs.langmuir.9b01900.

Characteristics of plasma proteins (PDF)

AUTHOR INFORMATION

Corresponding Author

*E-mail: jdriske@ilstu.edu.

ORCID

Jeremy D. Driskell: 0000-0001-5082-898X

Notes

The authors declare no competing financial interest.

ACKNOWLEDGMENTS

This work was supported by the Defense Threat Reduction Agency, Basic Research Award # HDTRA1-13-1-0028 and the National Science Foundation through the Macromolecular, Supramolecular and Nanochemistry Program, Award # CHE-1807126.

REFERENCES

(1) Dreaden, E. C.; Alkilany, A. M.; Huang, X.; Murphy, C. J.; El-Sayed, M. A. The golden age: gold nanoparticles for biomedicine. *Chem. Soc. Rev.* **2012**, *41*, 2740−2779.

(2) Dykman, L.; Khlebtsov, N. Gold nanoparticles in biomedical applications: recent advances and perspectives. *Chem. Soc. Rev.* **2012**, *41*, 2256−2282.

(3) Giljohann, D. A.; Seferos, D. S.; Daniel, W. L.; Massich, M. D.; Patel, P. C.; Mirkin, C. A. Gold Nanoparticles for Biology and Medicine. *Angew. Chem. Int. Ed.* **2010**, *49*, 3280−3294.

(4) Yeh, Y.-C.; Creran, B.; Rotello, V. M. Gold nanoparticles: preparation, properties, and applications in bionanotechnology. *Nanoscale* **2012**, *4*, 1871−1880.

(5) Li, W.; Chen, X. Gold nanoparticles for photoacoustic imaging. *Nanomedicine* **2015**, *10*, 299−320.

(6) Murphy, C. J.; Gole, A. M.; Stone, J. W.; Sisco, P. N.; Alkilany, A. M.; Goldsmith, E. C.; Baxter, S. C. Gold Nanoparticles in Biology: Beyond Toxicity to Cellular Imaging. *Acc. Chem. Res.* **2008**, *41*, 1721−1730.

(7) Ghosh, P.; Han, G.; De, M.; Kim, C. K.; Rotello, V. M. Gold nanoparticles in delivery applications. *Adv. Drug Deliv. Rev.* **2008**, *60*, 1307−1315.

(8) Ali, M. R. K.; Wu, Y.; El-Sayed, M. A. Gold-Nanoparticle-Assisted Plasmonic Photothermal Therapy Advances Toward Clinical Application. *J. Phys. Chem. C* **2019**, *123*, 15375.

(9) Zhou, W.; Gao, X.; Liu, D.; Chen, X. Gold Nanoparticles for In Vitro Diagnostics. *Chem. Rev.* **2015**, *115*, 10575−10636.

(10) Giljohann, D. A.; Seferos, D. S.; Patel, P. C.; Millstone, J. E.; Rosi, N. L.; Mirkin, C. A. Oligonucleotide Loading Determines Cellular Uptake of DNA-Modified Gold Nanoparticles. *Nano Lett.* **2007**, *7*, 3818−3821.

(11) Patel, P. C.; Giljohann, D. A.; Daniel, W. L.; Zheng, D.; Prigodich, A. E.; Mirkin, C. A. Scavenger Receptors Mediate Cellular Uptake of Polyvalent Oligonucleotide-Functionalized Gold Nanoparticles. *Bioconjugate Chem.* **2010**, *21*, 2250−2256.

(12) Alkilany, A. M.; Murphy, C. J. Toxicity and cellular uptake of gold nanoparticles: what we have learned so far? *J. Nanopart. Res.* **2010**, *12*, 2313−2333.

(13) Goodman, C. M.; McCusker, C. D.; Yilmaz, T.; Rotello, V. M. Toxicity of Gold Nanoparticles Functionalized with Cationic and Anionic Side Chains. *Bioconjugate Chem.* **2004**, *15*, 897−900.

(14) Amoozgar, Z.; Yeo, Y. Recent advances in stealth coating of nanoparticle drug delivery systems. *Wiley Interdiscip. Rev.: Nanomed. Nanobiotechnol.* **2012**, *4*, 219−233.

(15) Chen, Y.; Xu, Z.; Zhu, D.; Tao, X.; Gao, Y.; Zhu, H.; Mao, Z.; Ling, J. Gold nanoparticles coated with polysarcosine brushes to enhance their colloidal stability and circulation time in vivo. *J. Colloid Interface Sci.* **2016**, *483*, 201−210.

(16) Lévy, R.; Thanh, N. T. K.; Doty, R. C.; Hussain, I.; Nichols, R. J.; Schiffrin, D. J.; Brust, M.; Fernig, D. G. Rational and Combinatorial Design of Peptide Capping Ligands for Gold Nanoparticles. *J. Am. Chem. Soc.* **2004**, *126*, 10076−10084.

(17) Nowinski, A. K.; White, A. D.; Keefe, A. J.; Jiang, S. Biologically Inspired Stealth Peptide-Capped Gold Nanoparticles. *Langmuir* **2014**, *30*, 1864−1870.

(18) Kumar, A.; Ma, H.; Zhang, X.; Huang, K.; Jin, S.; Liu, J.; Wei, T.; Cao, W.; Zou, G.; Liang, X.-J. Gold nanoparticles functionalized

with therapeutic and targeted peptides for cancer treatment. *Biomaterials* **2012**, *33*, 1180−1189.
(19) Cedervall, T.; Lynch, I.; Lindman, S.; Berggard, T.; Thulin, E.; Nilsson, H.; Dawson, K. A.; Linse, S. Understanding the nanoparticle-protein corona using methods to quantify exchange rates and affinities of proteins for nanoparticles. *Proc. Natl. Acad. Sci. U. S. A.* **2007**, *104*, 2050−2055.
(20) Ke, P. C.; Lin, S.; Parak, W. J.; Davis, T. P.; Caruso, F. A Decade of the Protein Corona. *ACS Nano* **2017**, *11*, 11773−11776.
(21) Lacerda, S. H. D. P.; Park, J. J.; Meuse, C.; Pristinski, D.; Becker, M. L.; Karim, A.; Douglas, J. F. Interaction of Gold Nanoparticles with Common Human Blood Proteins. *ACS Nano* **2010**, *4*, 365−379.
(22) Walczyk, D.; Bombelli, F. B.; Monopoli, M. P.; Lynch, I.; Dawson, K. A. What the Cell "Sees" in Bionanoscience. *J. Am. Chem. Soc.* **2010**, *132*, 5761−5768.
(23) Hamad-Schifferli, K. Exploiting the novel properties of protein coronas: emerging applications in nanomedicine. *Nanomedicine* **2015**, *10*, 1663−1674.
(24) Mahon, E.; Salvati, A.; Baldelli Bombelli, F.; Lynch, I.; Dawson, K. A. Designing the nanoparticle−biomolecule interface for "targeting and therapeutic delivery". *J. Control Release* **2012**, *161*, 164−174.
(25) Maiorano, G.; Sabella, S.; Sorce, B.; Brunetti, V.; Malvindi, M. A.; Cingolani, R.; Pompa, P. P. Effects of Cell Culture Media on the Dynamic Formation of Protein−Nanoparticle Complexes and Influence on the Cellular Response. *ACS Nano* **2010**, *4*, 7481−7491.
(26) Goy-López, S.; Juárez, J.; Alatorre-Meda, M.; Casals, E.; Puntes, V. F.; Taboada, P.; Mosquera, V. Physicochemical Characteristics of Protein-NP Bioconjugates: The Role of Particle Curvature and Solution Conditions on Human Serum Albumin Conformation and Fibrillogenesis Inhibition. *Langmuir* **2012**, *28*, 9113−9126.
(27) Lundqvist, M.; Stigler, J.; Cedervall, T.; Berggård, T.; Flanagan, M. B.; Lynch, I.; Elia, G.; Dawson, K. The Evolution of the Protein Corona around Nanoparticles: A Test Study. *ACS Nano* **2011**, *5*, 7503−7509.
(28) Lundqvist, M.; Stigler, J.; Elia, G.; Lynch, I.; Cedervall, T.; Dawson, K. A. Nanoparticle size and surface properties determine the protein corona with possible implications for biological impacts. *Proc. Natl. Acad. Sci. U. S. A.* **2008**, *105*, 14265−14270.
(29) Casals, E.; Pfaller, T.; Duschl, A.; Oostingh, G. J.; Puntes, V. Time Evolution of the Nanoparticle Protein Corona. *ACS Nano* **2010**, *4*, 3623−3632.
(30) Davidson, A. M.; Brust, M.; Cooper, D. L.; Volk, M. Sensitive Analysis of Protein Adsorption to Colloidal Gold by Differential Centrifugal Sedimentation. *Anal. Chem.* **2017**, *89*, 6807−6814.
(31) Siriwardana, K.; Wang, A.; Vangala, K.; Fitzkee, N.; Zhang, D. Probing the Effects of Cysteine Residues on Protein Adsorption onto Gold Nanoparticles Using Wild-Type and Mutated GB3 Proteins. *Langmuir* **2013**, *29*, 10990−10996.
(32) Wang, A.; Vangala, K.; Vo, T.; Zhang, D.; Fitzkee, N. C. A Three-Step Model for Protein−Gold Nanoparticle Adsorption. *J. Phys. Chem. C* **2014**, *118*, 8134−8142.
(33) Frey, B. L.; Corn, R. M. Covalent attachment and derivatization of poly (L-lysine) monolayers on gold surfaces as characterized by polarization− modulation FT-IR spectroscopy. *Anal. Chem.* **1996**, *68*, 3187−3193.
(34) Grubisha, D. S.; Lipert, R. J.; Park, H.-Y.; Driskell, J.; Porter, M. D. Femtomolar detection of prostate-specific antigen: an immunoassay based on surface-enhanced Raman scattering and immunogold labels. *Anal. Chem.* **2003**, *75*, 5936−5943.
(35) Guler, Z.; Sarac, A. S. Electrochemical impedance and spectroscopy study of the EDC/NHS activation of the carboxyl groups on poly (ε-caprolactone)/poly (m-anthranilic acid) nanofibers. *eXPRESS Polym. Lett.* **2016**, *10*, 96.
(36) Jazayeri, M. H.; Amani, H.; Pourfatollah, A. A.; Pazoki-Toroudi, H.; Sedighimoghadam, B. Various methods of gold nanoparticles (GNPs) conjugation to antibodies. *Sens. Biosens. Res.* **2016**, *9*, 17−22.
(37) Raghav, R.; Srivastava, S. Immobilization strategy for enhancing sensitivity of immunosensors: L-Asparagine−AuNPs as a promising alternative of EDC−NHS activated citrate−AuNPs for antibody immobilization. *Biosens. Bioelectron.* **2016**, *78*, 396−403.
(38) Wagner, P.; Hegner, M.; Kernen, P.; Zaugg, F.; Semenza, G. Covalent immobilization of native biomolecules onto Au (111) via N-hydroxysuccinimide ester functionalized self-assembled monolayers for scanning probe microscopy. *Biophys. J.* **1996**, *70*, 2052−2066.
(39) Ciaurriz, P.; Fernández, F.; Tellechea, E.; Moran, J. F.; Asensio, A. C. Comparison of four functionalization methods of gold nanoparticles for enhancing the enzyme-linked immunosorbent assay (ELISA). *Beilstein J. Nanotechnol.* **2017**, *8*, 244.
(40) Filbrun, S. L.; Driskell, J. D. A fluorescence-based method to directly quantify antibodies immobilized on gold nanoparticles. *Analyst* **2016**, *141*, 3851−3857.
(41) Filbrun, S. L.; Filbrun, A. B.; Lovato, F. L.; Oh, S. H.; Driskell, E. A.; Driskell, J. D. Chemical Modification of Antibodies Enables the Formation of Stable Antibody-Gold Nanoparticle Conjugates for Biosensing. *Analyst* **2017**, *142*, 4456.
(42) Ruiz, G.; Tripathi, K.; Okyem, S.; Driskell, J. D. pH Impacts the Orientation of Antibody Adsorbed onto Gold Nanoparticles. *Bioconjugate Chem.* **2019**, *30*, 1182−1191.
(43) Vangala, K.; Ameer, F.; Salomon, G.; Le, V.; Lewis, E.; Yu, L.; Liu, D.; Zhang, D. Studying Protein and Gold Nanoparticle Interaction Using Organothiols as Molecular Probes. *J. Phys. Chem. C* **2012**, *116*, 3645−3652.
(44) Liu, F.; Wang, L.; Wang, H.; Yuan, L.; Li, J.; Brash, J. L.; Chen, H. Modulating the Activity of Protein Conjugated to Gold Nanoparticles by Site-Directed Orientation and Surface Density of Bound Protein. *ACS Appl. Mater. Interfaces* **2015**, *7*, 3717−3724.
(45) Driskell, J. D.; Jones, C. A.; Tompkins, S. M.; Tripp, R. A. One-Step Assay for Detecting Influenza Virus Using Dynamic Light Scattering and Gold Nanoparticles. *Analyst* **2011**, *136*, 3083−3090.
(46) Jans, H.; Huo, Q. Gold nanoparticle-enabled biological and chemical detection and analysis. *Chem. Soc. Rev.* **2012**, *41*, 2849−2866.
(47) Jans, H.; Liu, X.; Austin, L.; Maes, G.; Huo, Q. Dynamic Light Scattering as a Powerful Tool for Gold Nanoparticle Bioconjugation and Biomolecular Binding Studies. *Anal. Chem.* **2009**, *81*, 9425−9432.
(48) Lai, Y. H.; Koo, S.; Oh, S. H.; Driskell, E. A.; Driskell, J. D. Rapid screening of antibody−antigen binding using dynamic light scattering (DLS) and gold nanoparticles. *Anal. Methods* **2015**, *7*, 7249−7255.
(49) Liu, X.; Huo, Q. A washing-free and amplification-free one-step homogeneous assay for protein detection using gold nanoparticle probes and dynamic light scattering. *J. Immunol. Methods* **2009**, *349*, 38−44.
(50) Lopez, A.; Lovato, F.; Hwan Oh, S.; Lai, Y. H.; Filbrun, S.; Driskell, E. A.; Driskell, J. D. SERS immunoassay based on the capture and concentration of antigen-assembled gold nanoparticles. *Talanta* **2016**, *146*, 388−393.
(51) Mandl, A.; Filbrun, S. L.; Driskell, J. D. Asymmetrically Functionalized Antibody−Gold Nanoparticle Conjugates to Form Stable Antigen-Assembled Dimers. *Bioconjugate Chem.* **2017**, *28*, 38−42.
(52) Vroman, L.; Adams, A. L. Identification of rapid changes at plasma−solid interfaces. *J. Biomed. Mater. Res.* **1969**, *3*, 43−67.
(53) Monopoli, M. P.; Walczyk, D.; Campbell, A.; Elia, G.; Lynch, I.; Baldelli Bombelli, F.; Dawson, K. A. Physical-Chemical Aspects of Protein Corona: Relevance toin Vitroandin VivoBiological Impacts of Nanoparticles. *J. Am. Chem. Soc.* **2011**, *133*, 2525−2534.
(54) Filipe, V.; Hawe, A.; Jiskoot, W. Critical Evaluation of Nanoparticle Tracking Analysis (NTA) by NanoSight for the Measurement of Nanoparticles and Protein Aggregates. *Pharm. Res.* **2010**, *27*, 796−810.
(55) James, A. E.; Driskell, J. D. Monitoring gold nanoparticle conjugation and analysis of biomolecular binding with nanoparticle tracking analysis (NTA) and dynamic light scattering (DLS). *Analyst* **2013**, *138*, 1212−1218.
(56) Tsai, D.-H.; DelRio, F. W.; Keene, A. M.; Tyner, K. M.; MacCuspie, R. I.; Cho, T. J.; Zachariah, M. R.; Hackley, V. A.

DOI: 10.1021/acs.langmuir.9b01900
Langmuir 2019, 35, 10601−10609

Adsorption and Conformation of Serum Albumin Protein on Gold Nanoparticles Investigated Using Dimensional Measurements and in Situ Spectroscopic Methods. *Langmuir* **2011**, *27*, 2464−2477.
(57) Bekdemir, A.; Stellacci, F. A centrifugation-based physicochemical characterization method for the interaction between proteins and nanoparticles. *Nat. Commun.* **2016**, *7*, 13121.
(58) Shang, L.; Nienhaus, G. U. In Situ Characterization of Protein Adsorption onto Nanoparticles by Fluorescence Correlation Spectroscopy. *Acc. Chem. Res.* **2017**, *50*, 387−395.
(59) Treuel, L.; Brandholt, S.; Maffre, P.; Wiegele, S.; Shang, L.; Nienhaus, G. U. Impact of Protein Modification on the Protein Corona on Nanoparticles and Nanoparticle−Cell Interactions. *ACS Nano* **2013**, *8*, 503−513.
(60) Brewer, S. H.; Glomm, W. R.; Johnson, M. C.; Knag, M. K.; Franzen, S. Probing BSA Binding to Citrate-Coated Gold Nanoparticles and Surfaces. *Langmuir* **2005**, *21*, 9303−9307.
(61) Tripathi, K.; Driskell, J. D. Quantifying Bound and Active Antibodies Conjugated to Gold Nanoparticles: A Comprehensive and Robust Approach To Evaluate Immobilization Chemistry. *ACS Omega* **2018**, *3*, 8253−8259.
(62) de Puig, H.; Bosch, I.; Carré-Camps, M.; Hamad-Schifferli, K. Effect of the Protein Corona on Antibody-Antigen Binding in Nanoparticle Sandwich Immunoassays. *Bioconjugate Chem.* **2017**, *28*, 230−238.
(63) Granger, J. H.; Porter, M. D. The Case for Human Serum as a Highly Preferable Sample Matrix for Detection of Anthrax Toxins. *ACS Sens.* **2018**, *3*, 2303−2310.
(64) Zheng, T.; Finn, C.; Parrett, C. J.; Dhume, K.; Hwang, J. H.; Sidhom, D.; Strutt, T. M.; Li Sip, Y. Y.; McKinstry, K. K.; Huo, Q. A Rapid Blood Test To Determine the Active Status and Duration of Acute Viral Infection. *ACS Infect. Dis.* **2017**, *3*, 866−873.
(65) Casals, E.; Pfaller, T.; Duschl, A.; Oostingh, G. J.; Puntes, V. F. Hardening of the Nanoparticle−Protein Corona in Metal (Au, Ag) and Oxide (Fe3O4, CoO, and CeO2) Nanoparticles. *Small* **2011**, *7*, 3479−3486.
(66) Milani, S.; Baldelli Bombelli, F.; Pitek, A. S.; Dawson, K. A.; Rädler, J. ReversibleversusIrreversible Binding of Transferrin to Polystyrene Nanoparticles: Soft and Hard Corona. *ACS Nano* **2012**, *6*, 2532−2541.

DOI: 10.1021/acs.langmuir.9b01900
Langmuir 2019, 35, 10601−10609